

Article ID: 1001-3555(2015)06-0563-12

Influence of Preparation Technology on the Activities of Mn-Fe/ZSM-5 Catalysts for Selective Catalytic Reduction of NO with NH₃

GAO Rui-rui, LOU Xiao-rong, BAI Wen-jun, MU Wen-tao, LI Zhe*

(College of Chemistry and Chemical Engineering, Taiyuan University of Technology, Taiyuan 030024, China)

Abstract: A series of Mn-Fe/ZSM-5 catalysts were prepared for the selective catalytic reduction (SCR) of NO. Additionally, the effects of co-precipitation and impregnation methods, Fe precursors, and calcination temperatures on morphology, chemical composition, and the catalytic activity were investigated. The results indicated that Mn-Fe/ZSM-5 catalyst exhibited superior SCR activity and a broad active temperature range (120 ~ 300 °C) when prepared by the co-precipitation method using Fe(NO₃)₃ as precursor and calcining it at 300 °C. At 120 °C, the conversion of NO achieved 96.7%, and the NO conversion was always more than 95% in the temperature range 120 ~ 300 °C. X-ray diffraction, ammonia-temperature programmed desorption, X-ray photoelectron spectroscopy, scanning electron microscopy, transmission electron microscope, N₂-physisorption were used to characterized. Manganese and iron were mainly dispersed on the catalyst surface in the state of MnO₂-Mn₂O₃ and Fe₂O₃ respectively, as evidenced by the combined result of XRD and XPS. Specifically, when the superior Mn⁴⁺/Mn³⁺ ratio is 1.254 and the larger number and stronger intensity of acid sites, NH₃ adsorption and NO reduction activity is promoted evidently. These factors may be identified as the primary reasons for its high de NO_x activity for NH₃-SCR.

Key words: Mn-Fe/ZSM-5; nitric oxide; selective catalytic reduction; MnO₂-Mn₂O₃

CLC number: O643.3

Document code: A

The emission control of nitrogen oxides (NO_x) from stationary or mobile sources has been a major concern related to environmental issue and air quality. Undoubtedly, the direct transformation of nitrogen oxides (NO and NO₂) to N₂ is the ideal removal method. So far, the selective catalytic reduction of NO_x with NH₃ (NH₃-SCR) under oxygen-rich conditions has been recognized as the most effective and promising technique, which can be ascribed to its better sulfur tolerance, moderate catalytic properties, and low operation cost for stationary flue gas denitrogenation and automotive exhaust purification^[1-3]. The zeolite support provides acid sites for NH₃ adsorption. And the transition metals play a crucial role in catalyzing the

oxidation of NO and the subsequent formation of surface NO_x adsorption complexes. So transition metals supported on zeolite catalysts are promising alternative SCR catalysts for the removal of NO_x from automotive emissions^[4-5]. Manganese-based catalysts have drawn much attention, because they show good activity and N₂ selectivity for low-temperature NO reduction with NH₃, and the presence of defects sites of various Mn oxidation states^[6]. Manganese oxides have labile lattice oxygen and various oxidation states for Mnⁿ⁺ (i. e., MnO, MnO₂, Mn₂O₃, and Mn₃O₄), making them excellent candidates for redox reactions. Peña, et al.^[7] found that the excellent low-temperature SCR activity

Received date: 2015-10-21; **Revised date:** 2015-11-20.

Foundation: This work was supported by the National Natural Science Foundation of China (No. 21073131), Shanxi Provincial Science and Technology Projects (No. 20140313002-2), and State Key Laboratory Breeding Base of Coal Science and Technology Co-founded by Shanxi Province and the Ministry of Science and Technology, Taiyuan University of Technology (No. MKX201301) (国家自然科学基金项目(项目编号: 21073131), 山西省科技攻关项目(项目编号: 20140313002-2) 和煤科学与技术省部共建重点实验室培育基地开放课题基金资助项目(项目编号: MKX201301)).

First author: Gao Ruirui (1993-), Woman, master, Study on application and modification of the catalysts for the selective catalytic reduction of NO_x from diesel exhaust (高蕊蕊(1993-), 女, 硕士, 主要研究催化剂在柴油车尾气 NO_x 选择性催化还原中的应用与改性).

* **Corresponding author:** E-mail: lizhe@tyut.edu.cn.

of $\text{MnO}_x/\text{TiO}_2$ catalyst was due to the combination of lower calcination temperature, abundant Lewis acid sites, and relatively high surface concentration. On the other hand, Fe-containing zeolites, which are inexpensive and nontoxic, have also been studied extensively over the past decade owing to their remarkable catalytic activity and durability for NH_3 -SCRs^[8-11]. Generally, Fe-zeolite catalysts possess higher activity and N_2 selectivity under medium and high reaction temperatures (450 ~ 600 °C). However, their low-temperature activity is poor, and thus they cannot fully meet the practical requirements. Based on the advantages of Mn and Fe, Mn-Fe complex catalysts systems have received increasing attention recently in an effort to improve the low-temperature activity and widen the operating temperature range of SCR catalysts. Wu et al.^[12] reported that the introduction of Fe to Mn/TiO_2 catalyst can inhibit catalyst sintering and keep MnO_x in an amorphous state, thereby enhancing the activity of the catalyst. Long and his coworkers^[13] found that NO conversion on Fe-Mn catalyst prepared by the co-precipitation method was 74% at 80 °C. Qi and Yang^[14] also revealed that Fe and Mn mixed oxide catalysts facilitate SCR reactions. Therefore, the study of Mn-Fe complex catalyst systems for NH_3 -SCRs not only has high theoretical significance, but it also has certain reference value for practical application.

In a previous work, our group prepared a superior Mn/ZSM-5 catalyst that proved to have excellent low-temperature activity as an SCR of NO with NH_3 ^[15]. In the current study, a series of Mn-Fe/ZSM-5 catalysts were prepared and applied for NO reduction with NH_3 in the presence of O_2 . The effects of preparation methods, precursors, and calcination temperatures on the SCR performance, structure, bulk phase, and surface composition of the catalysts were investigated. All the catalysts were characterized by X-ray diffraction (XRD), ammonia-temperature programmed desorption (NH_3 -TPD), X-ray photoelectron spectroscopy (XPS), scanning electron microscopy (SEM), N_2 -physisorption, and transmission electron microscope (TEM).

1 Experimental section

1.1 Catalyst preparation

A series of Mn-Fe/ZSM-5 catalysts were prepared respectively by co-precipitation (CP) and impregnation (IM) using manganese acetate ($\text{Mn}(\text{CH}_3\text{COO})_2 \cdot 4\text{H}_2\text{O}$, AR, supplied by Damao Reagent[®], Tianjin, China) as precursor, HZSM-5 (Si/Al = 38, provided by Nankai University, Tianjin, China) as support and ammonia ($\text{NH}_3 \cdot \text{H}_2\text{O}$, AR, supplied by Hengxing[®], Tianjin, China) as precipitant with ferric nitrate ($\text{Fe}(\text{NO}_3)_3 \cdot 9\text{H}_2\text{O}$, AR, supplied by Kermel[®], Tianjin, China) or Ferric chloride (FeCl_3 , AR, supplied by Kermel[®], Tianjin, China) as Fe precursors and different calcination temperatures (300 or 500 °C). The metal contents were 10% Mn and 10% Fe.

For CP method, appropriate amount of manganese acetate and ferric nitrate or ferric chloride were dissolved in deionized water and mixed with HZSM-5 by magnetic stirring for 24 h at room temperature. Then a certain amount of ammonia was gradually added into the resulting solution until the pH of the solution reached 11. The resulting precipitate was filtered, dried at 110 °C overnight and calcined in air for 5 h at different temperatures.

For IM method, certain amount of manganese acetate and ferric nitrate were dissolved in deionized water and mixed with HZSM-5 by magnetic stirring for 24 h at room temperature, then the water was slowly evaporated in a water bath at 80 °C. The impregnated catalysts were dried at 110 °C overnight, followed by calcination at 300 °C in air for 5 h.

The samples were denoted as MFZ. For example, MFZ-CP-N-300 represents the catalyst prepared by CP method, using $\text{Fe}(\text{NO}_3)_3$ as Fe precursor and calcined at 300 °C. Prior to catalytic activity test, all the samples were pressed at a pressure of 18 MPa, and then crushed and sieved to a size of 0.450 ~ 0.280 mm mesh.

1.2 Catalyst characterization

X-ray diffraction patterns for all samples in the 2θ range $5^\circ \sim 75^\circ$ were collected on a Fangyuan DX-2700 diffractometer with a Ni filtered $\text{Cu K}\alpha$ radiation source

at beam voltage of 40 kV and beam current of 30 mA.

Ammonia-temperature programmed desorption data were collected on a Micromeritics Autochem FINE-SORB-3010 Automated Catalyst Characterization System. Each sample with 150 mg of finely ground powder was initially pretreated in a flow of pure He at 300 °C for 3 h, then cooled to 50 °C. The sample was treated with 30 mL/min of 15% NH₃/He. Subsequently, the sample was flushed with 40 mL/min of He for 1 h to remove weakly bound NH₃. Once a stable baseline by TCD had been achieved, the temperature was ramped from 85 °C to 700 °C at a rate of 10 °C/min.

X-ray photoelectron spectra were recorded on a Kratos XSAM800 multifunctional surface analysis photoelectron spectrometer (UK) using Al K α as radiation source at 180 W. The binding energies (BE) of C 1s, Mn 2p, Fe 2p and O 1s were measured. Charging effects were eliminated by correcting the observed spectra with the C 1s BE value of 284.8 eV. For all the measurements, an estimated error of 0.1 eV can be considered.

Nitrogen adsorption isotherms were obtained at 196 °C (liquid N₂ temperature) using a NOVA 2000e analyzer. The samples were pretreated at 300 °C for 3 h under vacuum. The specific surface areas of the samples were calculated using the BET method.

Transmission electron microscope (TEM, JEM-2100F) was applied for the detailed microstructure and metal particle size distribution of the catalysts. Samples were carried out by suspending powder in a small amount of ethanol, later it was dispersed with the aid of an ultrasonic bath.

The surface morphology of catalysts was observed on a ZEISS EVO MA15 scanning electron microscopy manufactured by Carl Zeiss Company. Prior to the SEM experiments, the samples were processed by spraying gold because their non-conductive properties.

1.3 Activity measurement

The SCR activity measurement was carried out in a fixed-bed quartz reactor (inner diameter 6 mm) at atmospheric pressure. The reaction conditions were as follows: 0.5 cm³ of sample, 600 ppm NO, 600 ppm NH₃, 4.5% O₂, balance with N₂, different total flow

rate. The inlet and effluent NO concentrations were continually monitored by using an on-line flue gas analyzer (KM9106 Quintox, Kane May International Limited). All the data were obtained after 60 min when the SCR reaction reached steady state. The NO conversion (η) was calculated as follows:

$$\eta(\%) = \frac{[\text{NO}_x]_{\text{in}} - [\text{NO}_x]_{\text{out}}}{[\text{NO}_x]_{\text{in}}} \times 100\% \quad (1)$$

Where NO_{in}(ppm) is the inlet NO concentration and NO_{out}(ppm) is the outlet NO concentration.

2 Results

2.1 SCR activity

Figure 1 compares the catalytic activities of Mn/ZSM-5 and Mn-Fe/ZSM-5 catalysts prepared using

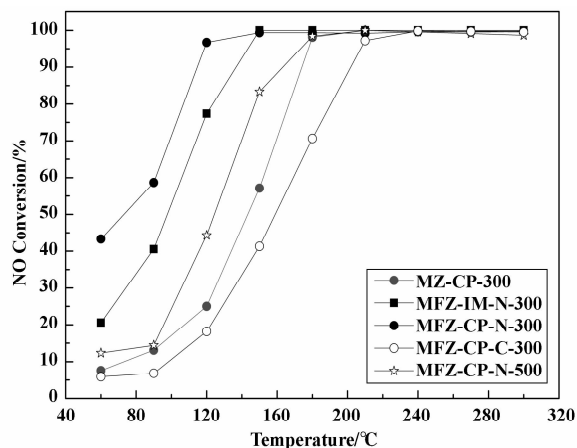


Fig. 1 NH₃-SCR activities of Mn/ZSM-5 and Mn-Fe/ZSM-5 catalysts prepared by different preparation technology

different preparation methods, Fe precursors, and calcination temperatures in terms of NO conversion as a function of reaction temperature in the reaction temperature range of 60 ~ 300 °C. The catalyst of MFZ-CP-N-300 revealed superior de NO_x activity in the low-temperature region. At 120 °C, it achieved 96.7% NO conversion as compared to 77.3% for the MFZ-IM-N-300 catalyst. The active temperature range of the MFZ-CP-N-300 catalyst was also broader than that of the other catalysts. In the temperature range 120 ~ 300 °C, the catalyst prepared with Fe(NO₃)₃ exhibited a NO conversion of more than 90%, whereas the catalyst prepared with FeCl₃ exhibited 90% NO conversion in

the range of 210 ~ 300 °C. According to the comparative analysis, the catalyst calcined at 500 °C (MFZ-CP-N-500) exhibited a much lower activity as compared to the catalyst calcined at 300 °C (MFZ-CP-N-300) in the low-temperature range (< 150 °C). When the reaction temperature exceeded 180 °C, the two catalysts showed similar NO conversion. Figure 2 shows the effect of the GHSV on NO conversion for MFZ-CP-N-300 at 120 °C. With the increase of the space velocity (GHSV), the NO conversion decreased monotonously. When the gas hourly space velocity decreased to 18 000 h⁻¹, NO has been converted into N₂ completely.

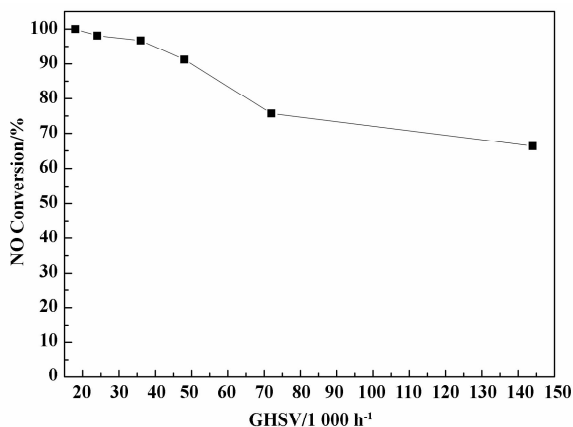


Fig. 2 NH₃-SCR activities of MFZ-CP-N-300 at 120 °C under different GHSV conditions

It is thus apparent that the NO_x activity of the Mn-Fe/ZSM-5 catalyst strongly depends on the preparation technology, and the Mn-Fe/ZSM-5 catalyst prepared by the CP method with Fe(NO₃)₃ as the precursor and calcined at 300 °C, i. e., MFZ-CP-N-300, shows the best low-temperature SCR activity and broadest active temperature range. The MFZ-CP-N-300 catalyst exhibited excellent stability, and NO conversion remained above 98% for a 120 h test at 300 °C.

2.2 XRD

The X-ray diffractograms of the HZSM-5 support and Mn-Fe/ZSM-5 catalysts prepared by different preparation technology are depicted in Figure 3. It can be seen that the commercial bulk HZSM-5 support contained strong and typical diffraction peaks at 2θ = 8°, 9°, 23°, and 24°^[16]. All the characteristic peaks corresponding to ZSM-5 can be observed for all the Mn-

Fe/ZSM-5 catalysts, suggesting that the implantation of metallic components during the preparation technology did not change the original structure of the carrier itself, whereas the intensities decreased dramatically as compared to the HZSM-5 support, indicating the strong interaction between ZSM-5 and metal oxides^[17-18].

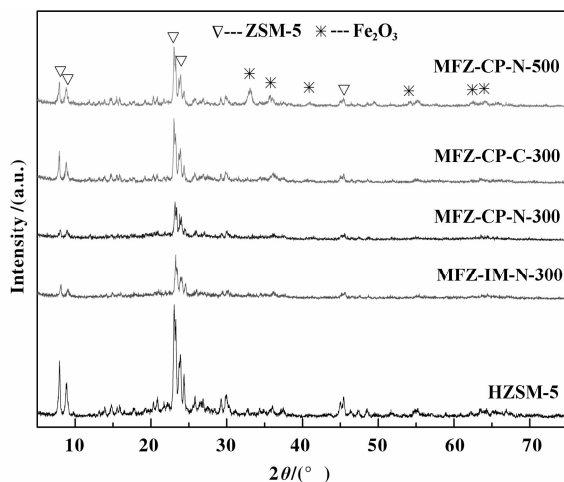


Fig. 3 XRD patterns of Mn-Fe/ZSM-5 catalysts prepared by different preparation technology

For the catalysts of MFZ-IM-N-300, MFZ-CP-N-300, and MFZ-CP-C-300, no visible iron or manganese oxide phase can be observed. This may be due to the low crystalline nature (amorphous) or the effective dispersion of metal oxides on the catalyst surface^[19-20]. The difference was that the ZSM-5 diffraction peak intensity of MFZ-N was lower than that of MFZ-C. The calcination temperature had a significant effect on the crystallinity of catalysts, and the strength of the ZSM-5 peaks increased with increasing calcination temperature. When the catalyst was calcined at 300 °C, no visible phase of Fe or Mn was observed, which may be due to the poor crystallinity or amorphous phase caused^[21]. However, when the calcination temperature increased to 500 °C, the diffraction peaks obtained at 2θ = 33°, 35.6°, 40.8°, 54°, 62.4°, and 64° can be assigned to Fe₂O₃ (JCPDF #33-0664)^[22], revealing the formation of crystalline Fe₂O₃ on the catalyst surface. Fe₂O₃ crystalline may result in the decrease of catalytic activity at low temperature.

2.3 NH₃-TPD

The catalyst surface acidity is also a critical factor

for the NH₃-SCR reaction. The large amount of the surface acidity of the Mn-Fe/ZSM-5 catalysts is maybe another reason for its excellent de NO_x activity. Differ-

ent categories of acid sites are listed in Table 1. The NH₃-TPD spectra of these catalysts contain at least two desorption peaks. The first peak is centered at about

Table 1 The surface acidity calculated from NH₃ desorption amount in NH₃-TPD

Sample	Acidity ^a /($\mu\text{mol} \cdot \text{m}_{\text{cat}}^{-2}$)	Low temperature		High temperature	
		T/($^{\circ}\text{C}$) ^b	L _{1/2} /($\mu\text{mol} \cdot \text{m}_{\text{cat}}^{-2}$)	T/($^{\circ}\text{C}$) ^b	L _{1/2} /($\mu\text{mol} \cdot \text{m}_{\text{cat}}^{-2}$)
MFZ-CP-N-300	9.1	197	5.5	413	3.6
MFZ-IM-N-300	8.9	195	5.4	400	3.5
MFZ-CP-N-500	6.8	175	5.8	390	1.0
MFZ-CP-C-300	4.6	162	3.4	315	1.2

a. Calculated from the specific NH₃ desorption amount per S_{BET} of the catalysts;

b. Central desorption temperature of the ammonia bound to different acid sites.

200 $^{\circ}\text{C}$, while the second one, much broader, at temperature about 400 $^{\circ}\text{C}$. The low temperature peak of 100 ~ 300 $^{\circ}\text{C}$ is present for all samples which is attributed to NH₃ desorbed by weak and medium acid sites either physisorbed or linked to weak Brønsted acid sites, while the high temperature peak of 300 ~ 500 $^{\circ}\text{C}$ can be attributed to NH₃ desorbed from chemisorbed or the strong Lewis acid sites. By comparing this kinds of catalysts, the second peak was shifted to higher temperature region from 315 to 413 $^{\circ}\text{C}$, gradually. The NH₃-TPD results demonstrate that the number and intensity of acid sites in the catalysts has a significant impact on the catalytic activity. As shown in the NH₃-TPD profiles of Figure 4, the MFZ-CP-N-300 catalyst

has a higher NH₃ adsorption capacity, compared to the other catalysts, mainly due to the large number of surface acidic sites on the ZSM-5 support and Mn-Fe bimetallic oxides. For these catalysts, the increased amount of Brønsted and strong Lewis acid is due to the MnO_x species. The NH₃ adsorption capacity in this study decreased in the following order: MFZ-CP-N-300 > MFZ-IM-N-300 > MFZ-CP-N-500 > MFZ-CP-C-300. And the intensity of acid sites catered to the activity order of the sample. Comparing the low temperature (393 K) SCR activity of our catalysts, it was concluded that catalysts having Lewis acidity were active and that Brønsted acidity may not be contributing to catalytic performance^[5].

2.4 XPS

To determine the surface atomic concentration and chemical states of Mn, Fe, and O in the surface region, XPS tests were conducted. The spectra of Mn 2p, Fe 2p, and O 1s are illustrated in Figure 5, and the binding energy and relative surface atomic concentration of Mn, Fe, and O obtained by XPS are listed of in Table 2, which also includes the area ratio of O_α/(O_α+O_β) and Mn⁴⁺/Mn³⁺ calculated by the corresponding characteristic peaks. As seen in Figure 5a, the spectra of Mn 2p display clear spin orbit-splitting peaks from 635 ~ 660 eV, assigned to Mn 2p_{3/2} and Mn 2p_{1/2} respectively, according to the X-ray photoelectron spectroscopy database of the National Institute

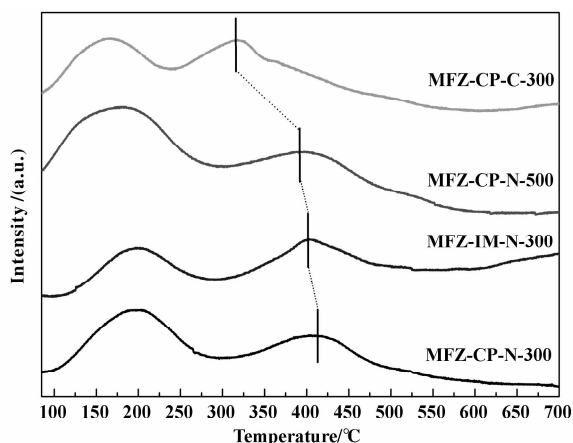


Fig. 4 NH₃-TPD over the catalysts; MFZ-CP-N-300, MFZ-IM-N-300, MFZ-CP-N-500, MFZ-CP-C-300

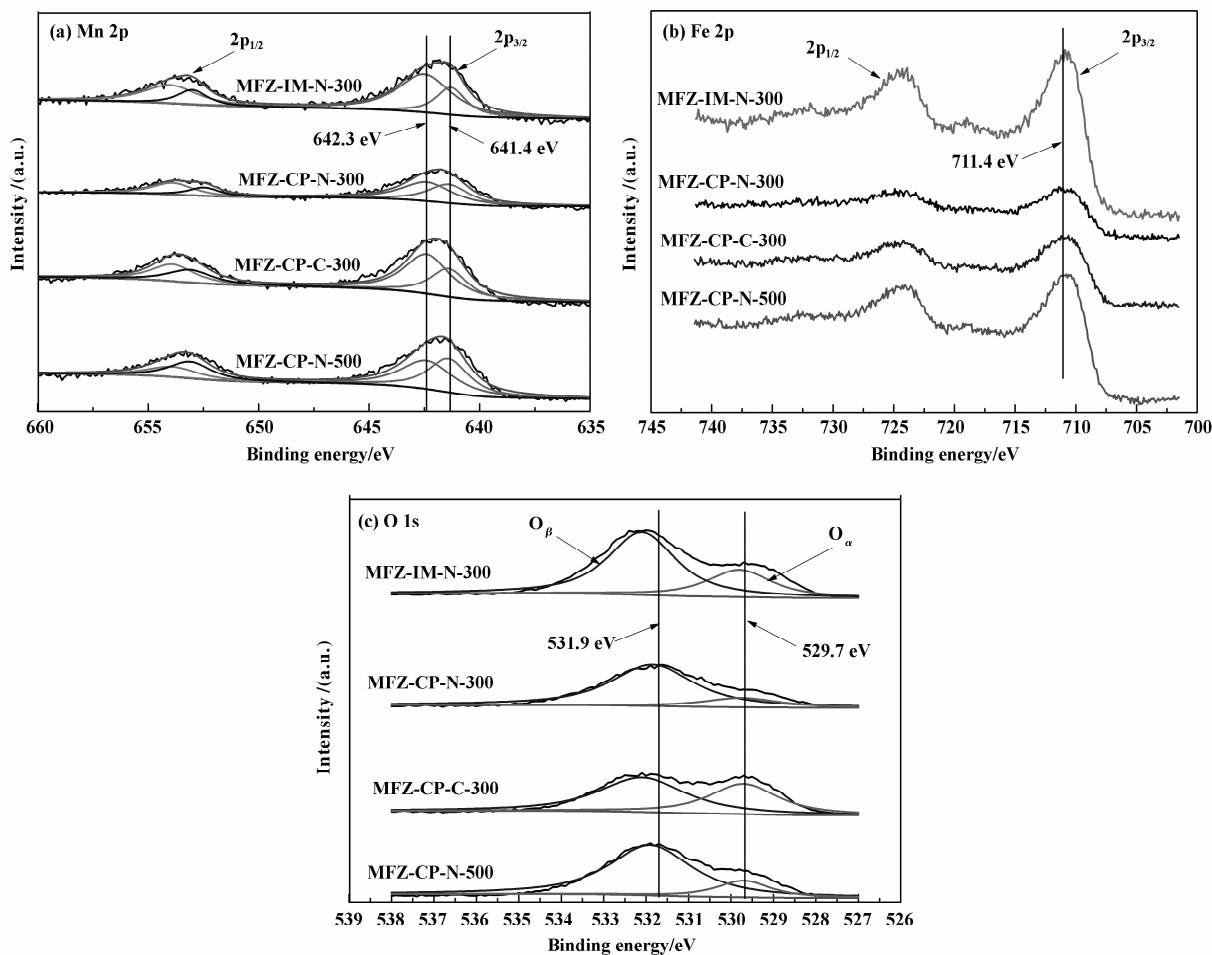


Fig. 5 XPS spectra of Mn 2p (a), Fe 2p (b), and O 1s (c)

Table 2 Binding energy and surface atomic concentration of Mn, Fe and O determined from XPS; MFZ-IM-N-300, MFZ-CP-N-300, MFZ-CP-N-500, MFZ-CP-C-300

Samples	Mn 2p/(eV)			Fe 2p/(eV)		O 1s/(eV)			Surface atomic composition/(atomic%)		
	2p _{1/2}	2p _{3/2}	Mn ⁴⁺ /Mn ³⁺	2p _{1/2}	2p _{3/2}	O _α	O _β	O _α /O _α +O _β	Mn	Fe	O
MFZ-IM-N-300	653.5	641.7	2.499	724.5	710.7	529.7	532.1	0.65	2.28	6.71	40.51
MFZ-CP-N-300	653.7	641.8	1.254	724.5	710.9	529.7	531.9	0.17	2.16	3.10	41.48
MFZ-CP-N-500	653.5	642.0	1.084	724.5	710.6	529.7	532.1	0.17	2.68	6.45	39.15
MFZ-CP-C-300	653.6	641.8	1.761	724.3	710.8	529.6	532.3	0.41	3.28	4.85	40.15

of Standards and Technology (NIST) and previous literature reports^[23–24]. For the identification of the surface manganese oxide phases and the relative percentages of Mn⁴⁺ and Mn³⁺ species, the overlapped Mn 2p peaks were deconvoluted into two peaks by searching for the optimal combination of Gaussian bands with the correlation coefficients (r^2) above 0.98. It has been

well established that the Mn⁴⁺ and Mn³⁺ peaks appear at 642.3 ± 0.1 eV and 641.4 ± 0.1 eV, respectively^[25]. Our XPS spectra of MnO₂, Mn₂O₃, Mn₃O₄, and MnO exhibited the Mn 2p_{3/2} peak near 642.3, 641.3, 641.4, and 641.5 eV, respectively^[25–26]. The deconvoluted peaks are signed as specific phases of manganese (MnO₂, Mn₂O₃) in each spectrum (Figure

5a). As shown in Table 2, the percent of Mn⁴⁺ cation on these Mn-Fe/ZSM-5 catalysts obviously varied. The Mn 2p_{3/2} binding energy of MFZ-CP-N-300 was about 641.8 eV, and the Mn⁴⁺/Mn³⁺ ratio was 1.254, indicating that the Mn species mainly existed in the form of MnO₂-Mn₂O₃, and some MnO₂ was transformed into Mn₂O₃^[27]. For the MFZ-CP-N-500 catalyst, however, the Mn 2p_{3/2} binding energy showed a increase of about 0.2 eV. This may have been due to an interaction between Mn and Fe. Moreover, the Mn⁴⁺/Mn³⁺ ratio decreased from 1.254 to 1.084, which suggested that the Mn species mainly existed in the form of Mn₂O₃. For the MFZ-CP-C-300 and MFZ-IM-N-300 catalyst, the Mn⁴⁺/Mn³⁺ ratio increased to 1.761 and 2.499, indicating that the MnO₂ was the main existence form, which strongly interacted with the support surface^[21,28-29]. Considering the SCR activity results, the ratio of MnO₂ and Mn₂O₃ on the surface of the catalysts may play an important role in determining the activity^[27]. As shown in Figure 5b, the Fe 2p spectra of the four catalysts exhibited a doublet corresponding to Fe 2p_{1/2} at 724.4 ± 0.1 eV and Fe 2p_{3/2} at 710.8 ± 0.1 eV, and these values are consistent with the reported values of Fe₂O₃^[30-31], proving that Fe with a valence of +3 likely existed on these catalysts.

The peak deconvolution and fitting procedure show that the O 1s peak is well fitted by two peaks as shown in Figure 5c, indicating that two kinds of surface oxygen species exist. The peak at 529.6 ~ 529.7 eV most

likely belongs to lattice oxygen (O²⁻, hereafter denoted as O_α) and the peak at 531.9 ~ 532.3 eV is related to the weakly surface-adsorbed oxygen ions with low coordination (O₂²⁻ and O⁻, hereafter denoted as O_β)^[18,28,32-33]. The binding energy of O_α mainly centered at about 529.7 eV, as expected for the transition metal oxides^[34]. Another oxygen species O_β at about 531.9 eV was also observed, which was assigned to -OH^[31]. Obviously, the catalyst prepared with FeCl₃ possessed more lattice oxygen species than that prepared with Fe(NO₃)₃ except MFZ-IM-N-300. When the calcination temperature increased from 300 to 500 °C, the ratio of O_α/(O_α+O_β) remained the same, indicating that the calcination temperature has little effect on the relative content of lattice oxygen species and surface-adsorbed oxygen species. The lattice oxygen plays an important role in the NH₃-SCR reaction. And it is considered to be the most active oxygen species. The reaction proceeds firstly via a consumption of active oxygen, then a transferring of lattice oxygen to active sites and subsequently the re-oxidation of reduced catalysts by gas-phase oxygen. So the excellent low temperature activity of the catalyst associated with the surface lattice oxygen, which may promote the adsorption and activation of reactants (NH₃ or NO) on the catalyst surface.

2.5 N₂ adsorption/desorption and TEM

Table 3 summarized the BET surface area, total pore volume, and average pore size of the samples.

Table 3 Textural properties of HZSM-5, MFZ-CP-N-300, MFZ-IM-N-300, MFZ-CP-N-500, and MFZ-CP-C-300

Sample	S _{BET} /(m ² · g ⁻¹)	Average pore size/nm	Total pore volume/(cm ³ · g ⁻¹)
HZSM-5	492.461	0.614	0.3007
MFZ-CP-N-300	348.461	0.666	0.2848
MFZ-IM-N-300	334.012	0.615	0.3684
MFZ-CP-N-500	299.123	0.682	0.2387
MFZ-CP-C-300	250.546	0.723	0.3495

The results indicated that the samples were typical microporous material (Figure 6a) and that after loading Mn and Fe the pore structure of ZSM-5 changed to some extent. The S_{BET} of these catalysts were affected

by the prepared technology and decreased from 348.461 m²g⁻¹ to 250.546 m²g⁻¹ monotonically. The decreased S_{BET} can be deemed to the blocking effect on pores arising from addition of metal oxide species

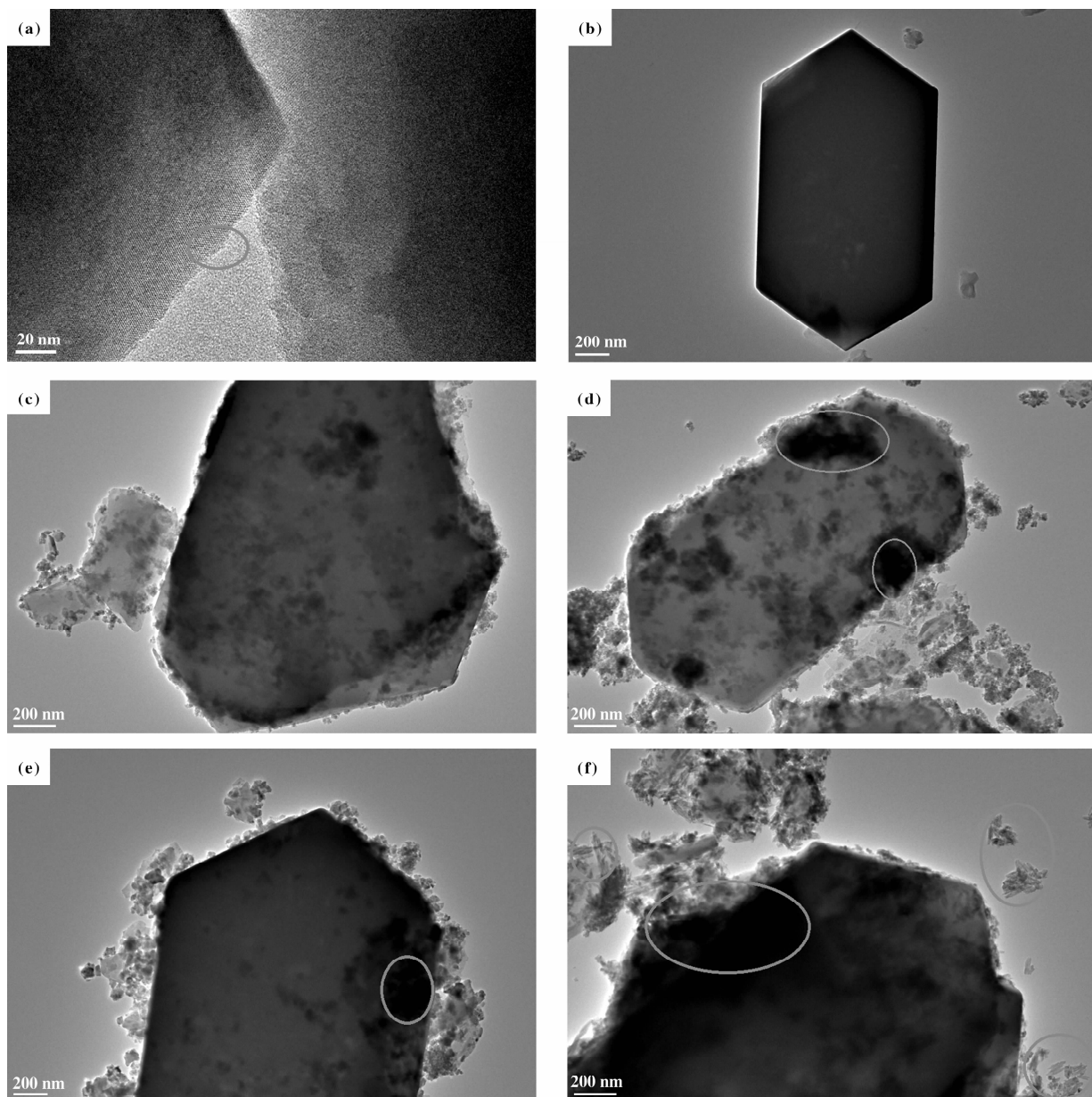


Fig. 6 TEM images and metal oxide particle distribution of HZSM-5 (a and b), MFZ-CP-N-300 (c), MFZ-IM-N-300 (d), MFZ-CP-N-500 (e), and MFZ-CP-C-300 (f)

(Figure 6). All the catalysts had similar isothermal to that of the HZSM-5 support, suggesting that all the catalysts retained the well microporous properties. Furthermore, co-precipitation and impregnation methods had little effect on the surface area of MFZ-CP-N-300 and MFZ-IM-N-300. The reason that MFZ-CP-N-300 increased the activity at low temperature might be independent of the surface area.

Figure 6 showed that TEM images and metal particle distribution of these samples. Figure 6a and b

showed the structure of ZSM-5 zeolite, with three-dimensional channel defined by 10-membered ring openings. It can be found that small and homogeneous metal particles were uniformly present over the MFZ-CP-N-300 and that the four catalysts were still maintained a good structure of the ZSM-5. Compared with the MFZ-CP-N-300, the sintering phenomenon of the other catalysts was more serious. Finally, the image of the MFZ-CP-C-300 catalyst showed strip material but without the structure of the ZSM-5, which might

reduced the catalytic activity. The results convince that prepared technology has a significant effect on the structure of the supported Mn and Fe particles.

2.6 SEM

Further insight into the influence of precursors and different temperatures on the structural features of the HZSM-5 support and the Mn-Fe/ZSM-5 catalysts come from the SEM graphs shown in Figure 7. The structure and morphology of HZSM-5 also have not been changed through modification. As indicated in Figure 7a, the surface of pure HZSM-5 was smooth. In contrast, the surface became rough after doping, and particles ten-

ded to clump and agglomerate to some extent, suggesting that active components had been supported on the surface of HZSM-5. By contrasting Figure 7b with Figure 7c, it can be seen that particles of MFZ-N were more uniform, and the aggregation of the particles was significantly lower than the MFZ-C particles. To a certain extent, this led to the decrease in the catalytic activity of MFZ-C. As shown in Figure 7d, the amorphous structure disappeared and obvious regular and smooth particles formed on the sample calcined at 500 °C, which is consistent with the previous XRD results.

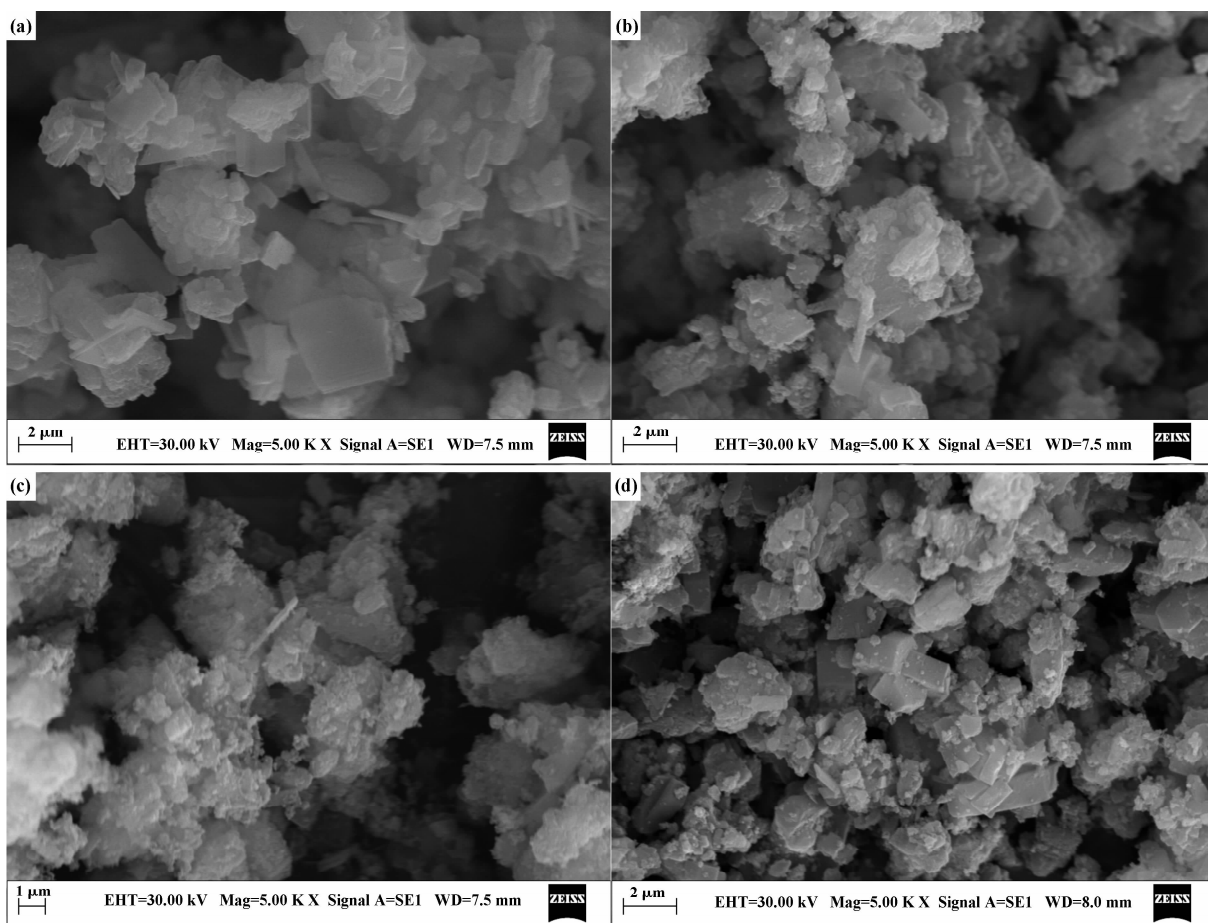


Fig. 7 SEM images of Mn-Fe/ZSM-5 catalysts prepared by different precursors and different temperatures: (a) HZSM-5, Mag = 5000x; (b) MFZ-CP-N-300, Mag = 5000x; (c) MFZ-CP-C-300, Mag = 5000x; (d) MFZ-CP-N-500, Mag = 5000x

3 Discussion

Due to a strong synergy between Mn and Fe, the appropriate Mn⁴⁺/Mn³⁺ ratio might have a great effect on the reduction of NO similar to the results that the

co-existence of Mn₂O₃ and MnO₂ enhanced the oxidation of NH₃ and contributed to the catalytic reaction at low temperature^[35]. It follows Langmuir-Hinshelwood mechanism at lower temperature. The SCR reaction can be approximately described as: NH₃ (g) ⇌ NH₃

(ad), $\text{NO}(\text{g}) \rightleftharpoons \text{NO}(\text{ad})$, $\text{Mn}^{4+} \cdot \text{O} + \text{NO}(\text{ad}) \rightarrow \text{Mn}^{3+} + \text{NO}_2^-$, $\text{NO}_2^- + \text{NH}_3 \rightarrow \text{N}_2 + \text{H}_2\text{O} + \text{OH}^-$, $\text{Mn}^{3+} + 1/4\text{O}_2 \rightarrow \text{Mn}^{4+} + 1/2\text{O}^{[34]}$. As described in the literature the ability of Fe^{3+} cation to oxidize NO to NO_2^- was much less than that of Mn^{4+} . Therefore, Fe^{3+} might be neglected if there were some Mn^{4+} cation on the surface. It is generally believed that NH_3 begins with Lewis acid adsorption of the catalyst at NH_3 -SCR reaction, then the catalytic dehydrogenate is occurred under the lattice oxygen or other surface oxygen species.

4 Conclusion

As described above, the preparation technology may play an important role in determining the activity. The Mn-Fe/ZSM-5 catalyst prepared by the CP method with the $\text{Fe}(\text{NO}_3)_3$ precursor and calcining it at 300 °C exhibited the best SCR activity within the scope of the study, which could be attributed to the coexistence of MnO_2 - Mn_2O_3 , the appropriate $\text{Mn}^{4+}/\text{Mn}^{3+}$ ratio and the enhanced redox activities. This was primarily due to the better dispersion of metal oxides, better redox characteristics, the larger number and stronger intensity of acid sites, the larger S_{BET} , and more surface-adsorbed oxygen. In the range of 120 ~ 300 °C, MFZ-CP-N-300 exhibited more than 90% NO conversion. And the MFZ-CP-N-300 catalyst had a good stability. Mn and Fe were properly dispersed on the catalyst surface and existed in the form of amorphous MnO_2 - Mn_2O_3 and Fe_2O_3 , which was detrimental to the low-temperature SCR of NO_x . The presence of surface nitrate species under moderate calcination conditions may play a favorable role in the low-temperature SCR of NO_x with NH_3 . However, the mechanism of enhancing activity through nitrate species is still poorly understood and must be investigated in future research. This catalyst was made up of closely packed particles with regular morphology. The catalyst particles were relatively uniform and the surface oxygen species were mainly composed of adsorption oxygen species.

Acknowledgements:

This work is financially supported by the National Natural Science Foundation of China (No. 21073131), State Key Laboratory Breeding Base of

Coal Science and Technology Co-founded by Shanxi Province and the Ministry of Science and Technology, Taiyuan University of Technology (No. MKX201301) and the Key Technologies R&D Program of Shanxi Province of China (No. 20140313002-2).

References:

- [1] a. Bosch H, Janssen F. Formation and control of nitrogen oxides[J]. *Catal Today*, 1988, **2**(4): 369-379.
 - b. Zong Yue(宗玥), Li Meng-li(李孟丽), Yang Xiaolong(杨晓龙), et al. Ru supported on foamed aluminum applied in the low-temperature catalytic decomposition of N_2O (泡沫铝负载钌基催化剂应用于 N_2O 的低温催化分解研究) [J]. *J Mol Catal(China)*(分子催化), 2014, **28**(4): 336-343.
 - c. Wang Jian(王建), Zhang Hai-jie(张海杰), Xu Xiu-fen(徐秀峰). Catalytic decomposition of N_2O over $\text{Cu}_x\text{Fe}_{1-x}\text{Fe}_2\text{O}_4$ and $\text{Ni}_x\text{Fe}_{1-x}\text{Fe}_2\text{O}_4$ composite oxides(N_2O 在 $\text{Cu}_x\text{Fe}_{1-x}\text{Fe}_2\text{O}_4$ 和 $\text{Ni}_x\text{Fe}_{1-x}\text{Fe}_2\text{O}_4$ 复合氧化物催化剂上的分解反应) [J]. *J Mol Catal(China)*(分子催化), 2015, **29**(1): 75-81.
 - d. Wang Jian(王建), Dou Zhe(窦喆), Pan Yan-fei(潘燕飞), et al. Catalytic decomposition of N_2O over $\text{Mn}_x\text{Co}_{3-x}\text{O}_4$ mixed oxides and modified catalysts ($\text{Mn}_x\text{Co}_{3-x}\text{O}_4$ 复合氧化物及改性催化剂催化分解 N_2O) [J]. *J Mol Catal(China)*(分子催化), 2015, **29**(3): 246-255.
- [2] a. Armor J N. Environmental catalysis [J]. *Appl Catal B: Environ*, 1992, **1**(4): 221-256.
 - b. Feng Yu(封煜), Liu Xin-yong(刘新勇), Jiang Zhi(江治), et al. Photocatalysis activity of Pt/ TiO_2 toward low concentration NO abatement(TiO_2 负载 Pt 对光催化去除低浓度 NO 性能的影响) [J]. *J Mol Catal(China)*(分子催化), 2013, **27**(1): 76-82.
 - c. Yu Hua-liang(俞华良), Chen Ming-xia(陈铭夏), Zou Gu-chu(邹谷初), et al. Simultaneously catalytic removal of diesel particulates and NO_x on K/LiCoO₂ catalysts (K/LiCoO₂ 的制备及其同时催化去除碳烟和 NO_x 的性能研究) [J]. *J Mol Catal(China)*(分子催化), 2013, **27**(1): 49-54.
 - d. Li Hui-juan(李惠娟), Jiang Xiao-yuan(蒋晓原), Zheng Xiao-ming(郑小明). Non-thermal-plasmacombined with selective catalytic reaction of NO by CH_4 over CuO/CeO_2 - TiO_2/γ - Al_2O_3 catalyst (介质阻挡等离子体放电辅助 CuO/CeO_2 - TiO_2/γ - Al_2O_3 催化剂脱除 NO 的研究) [J]. *J Mol Catal(China)*(分子催化), 2014,

- 28**(2): 157-164.
- [3] a. Fedeyko J M, Chen B, Chen H-Y. Mechanistic study of the low temperature activity of transition metal exchanged zeolite SCR catalysts [J]. *Catal Today*, 2010, **151**(3/4): 231-236.
b. Liu Peng-fei(刘鹏飞), Lou Xiao-rong(娄晓荣), He Kai(何凯), *et al.* Effects of surfactants on the structure and catalytic performance of Fe-Mn/ZSM-5/CC monolithic honeycomb catalyst(表面活性剂对 Fe-Mn/ZSM-5/CC 整体式催化剂结构及 NO_x 催化还原性能的影响) [J]. *J Mol Catal(China)*(分子催化), 2014, **28**(3): 227-233.
- [4] Nedyalkova R, Shwan S, Skoglundh M, *et al.* Improved low-temperature SCR activity for Fe-BEA catalysts by H₂-pretreatment [J]. *Appl Catal B: Environ*, 2013, **138/139**: 373-380.
- [5] Suib S L. Microporous manganese oxides [J]. *Curr Opin Sol State & Mater Sci*, 1998, **3**(1): 63-70.
- [6] Peña D A, Uphade B S, Smirniotis P G. TiO₂-supported metal oxide catalysts for low-temperature selective catalytic reduction of NO with NH₃: I. Evaluation and characterization of first row transition metals [J]. *J Catal*, 2004, **221**(2): 421-431.
- [7] Long R Q, Yang R T. Superior Fe-ZSM-5 catalyst for selective catalytic reduction of nitric oxide by ammonia [J]. *J Amer Chem Soc*, 1999, **121**(23): 5595-5596.
- [8] Ma A Z, Grunert W. Selective catalytic reduction of NO by ammonia over Fe-ZSM-5 catalysts [J]. *Chem Commun*, 1999, **1999**(1): 71-72.
- [9] Schwidder M, Kumar M S, Klementiev K, *et al.* Selective reduction of NO with Fe-ZSM-5 catalysts of low Fe content: I. Relations between active site structure and catalytic performance [J]. *J Catal*, 2005, **231**(2): 314-330.
- [10] Delahay G, Valade D, Guzman-Vargas A, *et al.* Selective catalytic reduction of nitric oxide with ammonia on Fe-ZSM-5 catalysts prepared by different methods [J]. *Appl Catal B: Environ*, 2005, **55**(2): 149-155.
- [11] Wu Z B, Jiang B Q, Liu Y. Effect of transition metals addition on the catalyst of manganese/titania for low-temperature selective catalytic reduction of nitric oxide with ammonia [J]. *Appl Catal B: Environ*, 2008, **79**(4): 347-355.
- [12] Long R Q, Yang R T, Chang R. Low temperature selective catalytic reduction (SCR) of NO with NH₃ over Fe-Mn based catalysts [J]. *Chem Commun*, 2002, **2002**(5): 452-453.
- [13] Qi G, Yang R T. Low-temperature selective catalytic reduction of NO with NH₃ over iron and manganese oxides supported on titania [J]. *Appl Catal B: Environ*, 2003, **44**(3): 217-225.
- [14] Lou X R, Liu P F, Li J, *et al.* Effects of calcination temperature on Mn species and catalytic activities of Mn/ZSM-5 catalyst for selective catalytic reduction of NO with ammonia [J]. *Appl Surf Sci*, 2014, **307**: 382-387.
- [15] Li Z, Xie K-C, Huang W, *et al.* Selective catalytic reduction of NO_x with ammonia over Fe-Mo/ZSM-5 catalysts [J]. *Chem Engin & Technol*, 2005, **28**(7): 797-801.
- [16] Wang L S, Huang B C, Su Y X, *et al.* Manganese oxides supported on multi-walled carbon nanotubes for selective catalytic reduction of NO with NH₃: Catalytic activity and characterization [J]. *Chem Engin J*, 2012, **192**: 232-241.
- [17] Lv G, Bin F, Song C L, *et al.* Promoting effect of zirconium doping on Mn/ZSM-5 for the selective catalytic reduction of NO with NH₃ [J]. *Fuel*, 2013, **107**: 217-224.
- [18] Lin Q C, Li J H, Ma L, *et al.* Selective catalytic reduction of NO with NH₃ over Mn-Fe-USY under lean burn conditions [J]. *Catal Today*, 2010, **151**(3/4): 251-256.
- [19] Panahi P N, Salari D, Niaei A, *et al.* NO reduction over nanostructure M-Cu/ZSM-5 (M: Cr, Mn, Co and Fe) bimetallic catalysts and optimization of catalyst preparation by RSM [J]. *J Indus Engin Chem*, 2013, **19**(6): 1793-1799.
- [20] Park E, Le H A, Kim Y S, *et al.* Preparation and characterization of Mn₂O₃/TiO₂ nanomaterials synthesized by combination of CVC and impregnation method with different Mn loading concentration [J]. *Mater Res Bull*, 2012, **47**(4): 1040-1044.
- [21] Huang J H, Tong Z Q, Huang Y, *et al.* Selective catalytic reduction of NO with NH₃ at low temperatures over iron and manganese oxides supported on mesoporous silica [J]. *Appl Catal B: Envir*, 2008, **78**(3/4): 309-314.
- [22] Kang M, Park E D, Kim J M, *et al.* Manganese oxide catalysts for NO_x reduction with NH₃ at low temperatures [J]. *Appl Catal A: Gener*, 2007, **327**(2): 261-269.
- [23] Raj A M E, Victoria S G, Jothy V B, *et al.* XRD and XPS characterization of mixed valence Mn₃O₄ hausmanite thin films prepared by chemical spray pyrolysis technique [J]. *Appl Surf Sci*, 2010, **256**(9): 2920-2926.

- [24] Kim Y J, Kwon H J, Heo I, *et al.* Mn-Fe/ZSM5 as a low-temperature SCR catalyst to remove NO_x from diesel engine exhaust[J]. *Appl Catal B: Environ*, 2012, **126**: 9–21.
- [25] Fang D, Xie J L, Hu H, *et al.* Identification of MnO_x species and Mn valence states in MnO_x/TiO₂ catalysts for low temperature SCR[J]. *Chem Engin J*, 2015, **271**: 23–30.
- [26] Li J, Yang C W, Zhang Q, *et al.* Effects of Fe addition on the structure and catalytic performance of mesoporous Mn/Al-SBA-15 catalysts for the reduction of NO with ammonia[J]. *Catal Commun*, 2015, **62**: 24–28.
- [27] Shen B X, Zhang X P, Ma H Q, *et al.* A comparative study of Mn/CeO₂, Mn/ZrO₂ and Mn/Ce-ZrO₂ for low temperature selective catalytic reduction of NO with NH₃ in the presence of SO₂ and H₂O[J]. *J Environ Sci-Chin*, 2013, **25**(4): 791–800.
- [28] Qi G S, Yang R T. Characterization and FTIR studies of MnO_x-CeO₂ catalyst for low-temperature selective catalytic reduction of NO with NH₃ [J]. *J Phys Chem B*, 2004, **108**(40): 15738–15747.
- [29] Long R Q, Yang R T. Characterization of Fe-ZSM-5 catalyst for selective catalytic reduction of nitric oxide by ammonia[J]. *J Catal*, 2000, **194**(1): 80–90.
- [30] Kim Y J, Kwon H J, Heo I, *et al.* MnFe/ZSM5 as a low-temperature SCR catalyst to remove NO_x from diesel engine exhaust[J]. *Appl Catal B: Environ*, 2012, **126**: 9–21.
- [31] Wu Z B, Jin R B, Liu Y, *et al.* Ceria modified MnO_x/TiO₂ as a superior catalyst for NO reduction with NH₃ at low-temperature [J]. *Catal Commun*, 2008, **9**(13): 2217–2220.
- [32] Wu Y S, Zhang Y X, Liu M, *et al.* Complete catalytic oxidation of o-xylene over Mn-Ce oxides prepared using a redox-precipitation method[J]. *Catal Today*, 2010, **153**(3/4): 170–175.
- [33] Yang S J, Wang C Z, Li J H, *et al.* Low temperature selective catalytic reduction of NO with NH₃ over Mn-Fe spinel: Performance, mechanism and kinetic study[J]. *Appl Catal B: Environ*, 2011, **110**: 71–80.
- [34] Ding Z Y, Li L X, Wade D, *et al.* Supercritical water oxidation of NH₃ over a MnO₂/CeO₂ catalyst[J]. *Indus & Engin Chem Res*, 1998, **37**(5): 1707–1716.

制备工艺对 Mn-Fe/ZSM-5 催化剂在 NH₃ 选择催化还原 NO 反应中催化性能的影响

高蕊蕊, 娄晓荣, 白文君, 牟文涛, 李 哲*

(太原理工大学 化学化工学院, 山西 太原 030024)

摘要: 分别采用共沉淀法和浸渍法、不同铁前驱物以及不同焙烧温度等研究了制备工艺对 Mn-Fe/ZSM-5 催化剂的结构、化学组分及 NH₃-SCR 活性的影响. 结果显示, 当采用 Fe(NO₃)₃ 作为 Fe 前驱物, 并用共沉淀法制备、300 °C 焙烧条件下得到的 MFZ-CP-N-300 样品低温活性最优, 在 120 °C 时, 其 NO 的转化率达到 96.7%, 120 ~ 300 °C 范围内 NO 转化率始终保持在 95% 以上. 同时利用 XRD、NH₃-TPD、XPS、SEM、TEM、氮吸附等手段对催化剂结构、晶相、酸位、锰铁氧化物的化学形态及表面的形貌特征进行表征分析. 结果表明锰铁氧化物分别以 MnO₂-Mn₂O₃ 和 Fe₂O₃ 的形式高度分散于催化剂表面, 特别是当 Mn⁴⁺/Mn³⁺ 比例为 1.254 时, 有较强的表面中强酸和较多的酸位数, 从而增加了 NH₃ 的吸附能力, 提高 NO 的转化率.

关键词: Mn-Fe/ZSM-5; 氮氧化物; 选择性催化还原; MnO₂-Mn₂O₃